Computational Studies on the Kinetics and Mechanisms for NH_3 Reactions with ClO_x (x = 0−4) Radicals

Z. F. Xu and M. C. Lin*

Department of Chemistry, Emory University, Atlanta, Georgia 30322

Received: August 21, 2006; In Final Form: November 9, 2006

Kinetics and mechanisms for NH_3 reactions with ClO_x (x = 0−4) radicals have been investigated at the G2M level of theory in conjunction with statistical theory calculations. The geometric parameters of the species and stationary points involved in the reactions have been optimized at the B3LYP/6-311+G(3df,2p) level of theory. Their energetics have been further refined with the G2M method. The results show that the H-abstraction process is the most favorable channel in each reaction and the barriers predicted in decreasing order are OClO > ClO > Cl > ClO_3 > ClO_4. All reactions were found to occur by hydrogen-bonding complexes; the rate constants for these complex metathetical processes have been calculated in the temperature range 200−2000 K by the microcanonical VTST and/or RRKM theory (for ClO_4 + NH_3) with Eckart tunneling and multiple reflection corrections. The predicted rate constants are in good agreement with the available experimental data.

I. Introduction

The reactions of NH_3 with chain-carriers such as ClO_x (x = 0−4) radicals play a pivotal role in the propulsion kinetics of the systems containing ammonium perchlorate (AP), a widely used propellant at present.[1] These reactions may also be relevant to the chemistry of stratosphere and the explosion caused by ammonium perchlorate at the Pacific Engineering and Production Company (PEPCON) facility,[2] where some of these species are present.

In 1974, Clyne and Watson[3] studied mass spectrometrically the kinetics of rapid bimolecular reactions involving ClO ($X^2\Pi$, $v = 0$) radicals at 298 K using molecular beam sampling from a discharge-flow system. They found that the ClO radical is unreactive toward a range of singlet ground state molecules up to 670 K and estimated that the upper limit for the NH_3 + ClO rate constant at 670 K is 1×10^{-15} cm^3 molecule^{-1} s^{-1}. In 1977, Westenberg and DeHaas[4] reported their measurement for the $NH_3 + Cl \rightarrow NH_2 + HCl$ reaction with the rate constant of 1.23×10^{-13} cm^3 molecule^{-1} s^{-1} at 298 K and 19.6−43.8 Torr argon pressure by the flash photolysis−resonance fluorescence technique. Recently, Gao et al.[5] measured the rate constant for $Cl + NH_3 \rightarrow HCl + NH_2$ over 290−570 K by the time-resolved resonance fluorescence technique. The rate constant was fitted by the expression $k(NH_3 + Cl) = (1.08 \pm 0.05) \times 10^{-11}$ exp[−(2.74 ± 0.04 kcal mol^{-1})/RT] cm^3 molecule^{-1} s^{-1}. They also characterized the potential energy surface of this reaction with the composite G3B3, CBS-QB3, and MPWB1K density functional theory. To our knowledge, no other measurements nor theoretical studies on the kinetics and mechanisms for the ClO_x radical reactions with NH_3 have been reported. These reactions are in fact very relevant to the understanding and simulation of AP propulsion chemistry.

In the present study, the G2M method[6] has been employed to investigate the five reaction systems of NH_3 + ClO_x (x = 0−4), and their rate constants were also calculated and compared with the available experimental values.

II. Computational Methods

The geometric parameters of the species and stationary points related to the title reactions were optimized at the B3LYP/6-311+G(3df,2p) level of theory,[7] and their vibrational frequencies were also calculated at this level. For more accurate evaluation of the energetic parameters, higher-level single-point energy calculations of the stationary points were carried out by the modified Gaussian-2 (G2M) theory,[6] based on the optimized geometries at the B3LYP/6-311+G(3df,2p) level of theory. The G2M(CC2) method calculates the base energy at the PMP4/6-311G(d,p) level of theory and improves it with the expanded basis set and coupled cluster corrections as well as a "higher level correction (HLC)". All ab initio calculations were carried out with Gaussian 03 program.[8]

The rate constants for the five reactions were calculated by the VARIFLEX code[9] based on the microcanonical variational transition state (VTST) or Rice−Ramsperger−Kassel−Marcus (RRKM) theory[10] for processes which occur by stable intermediates. The component rates were evaluated at the E/J-resolved level, and the pressure dependence was treated by one-dimensional master equation calculations using the Boltzmann probability of the complex for the J-distribution. For the barrierless association/decomposition process, the fitted Morse function, $V(R) = D_e\{1 - \exp[-\beta(R - R_e)]\}^2$, was used to represent the minimum potential energy path (MEP) as will be discussed later. Here, D_e is the bonding energy excluding zero-point vibrational energy for an association reaction, R is the reaction coordinate (i.e., the distance between the two bonding atoms), and R_e is the equilibrium value of R at the stable intermediate structure. For the ClO_4 + NH_3 reaction which occurs via two rather deep prereaction and postreaction complexes (vide infra), we have also employed the ChemRate code of Mokrushin et al.[11] to corroborate the predicted rate constant by the Variflex program.[9]

* Corresponding author. E-mail: chemmcl@emory.edu. NSC Distinguished Visiting Professor at National Chiao Tung University, Hsinchu, Taiwan.

10.1021/jp065397t CCC: $37.00
Published on Web 01/04/2007

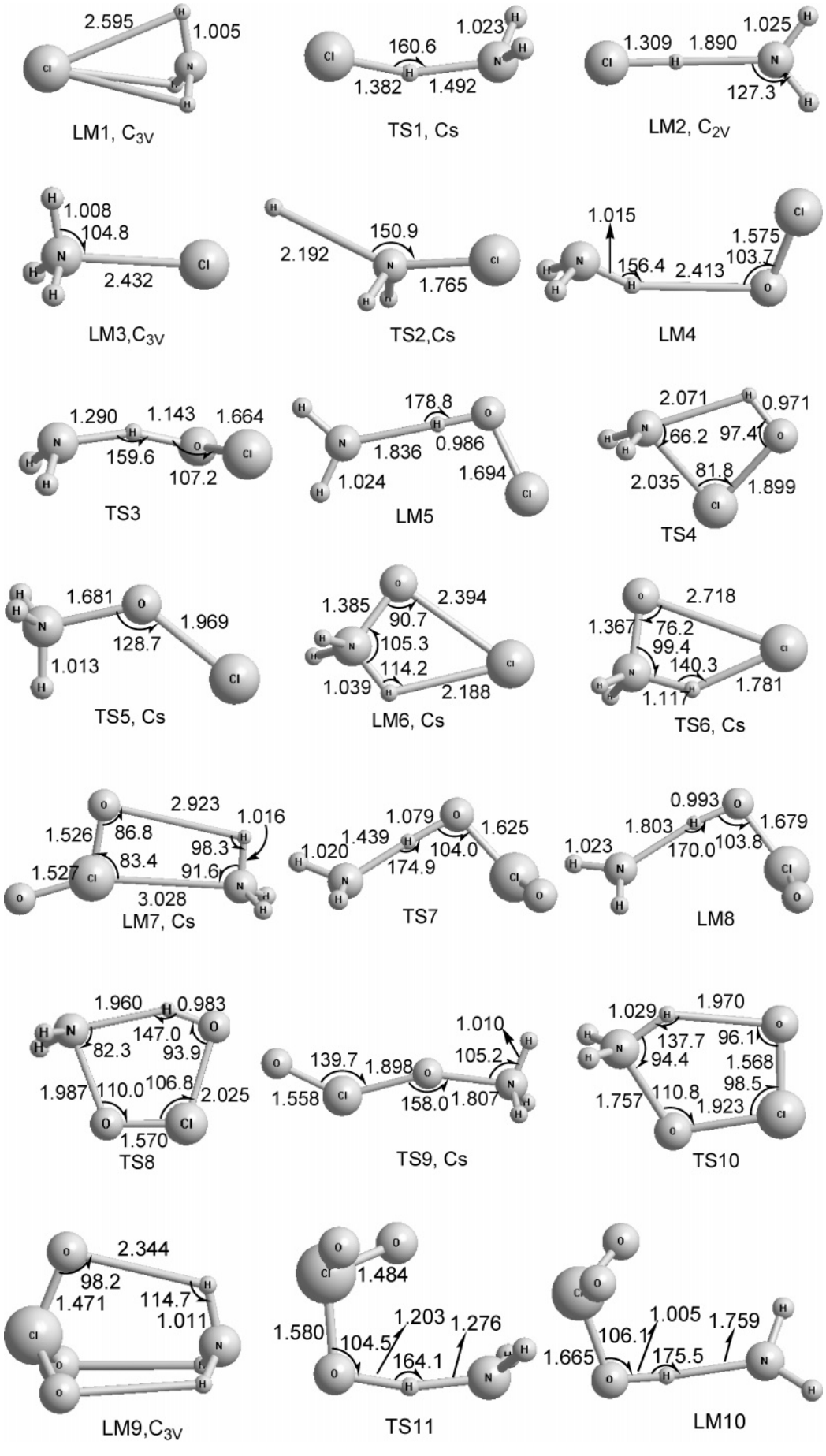
2.595
1.005
LM1, C3V
1.023
160.6
1.382
1.492
TS1, Cs
1.309
1.890
1.025
127.3
LM2, C2V
1.008
104.8
2.432
LM3,C3V
150.9
2.192
1.765
TS2,Cs
1.015
1.575
103.7
156.4
2.413
LM4
1.290
1.143
1.664
159.6
107.2
TS3
178.8
1.836
0.986
1.024
1.694
LM5
2.071
0.971
66.2
97.4
2.035
81.8
1.899
TS4
1.681
1.969
128.7
1.013
TS5, Cs
1.385
2.394
90.7
105.3
114.2
1.039
2.188
LM6, Cs
2.718
1.367
76.2
99.4
140.3
1.781
1.117
TS6, Cs
2.923
1.016
1.526
86.8
98.3
83.4
1.527
91.6
3.028
LM7, Cs
1.079
1.625
1.439
1.020
104.0
174.9
TS7
0.993
1.679
1.803
170.0
103.8
1.023
LM8
1.960
0.983
147.0
82.3
93.9
1.987
110.0
106.8
2.025
1.570
TS8
1.010
139.7
1.898
105.2
1.558
158.0
1.807
TS9, Cs
1.029
1.970
137.7
96.1
94.4
1.568
98.5
1.757
110.8
1.923
TS10
2.344
98.2
1.471
114.7
1.011
LM9,C3V
1.484
1.203
1.276
1.580
104.5
164.1
TS11
1.005
1.759
106.1
1.665
175.5
LM10

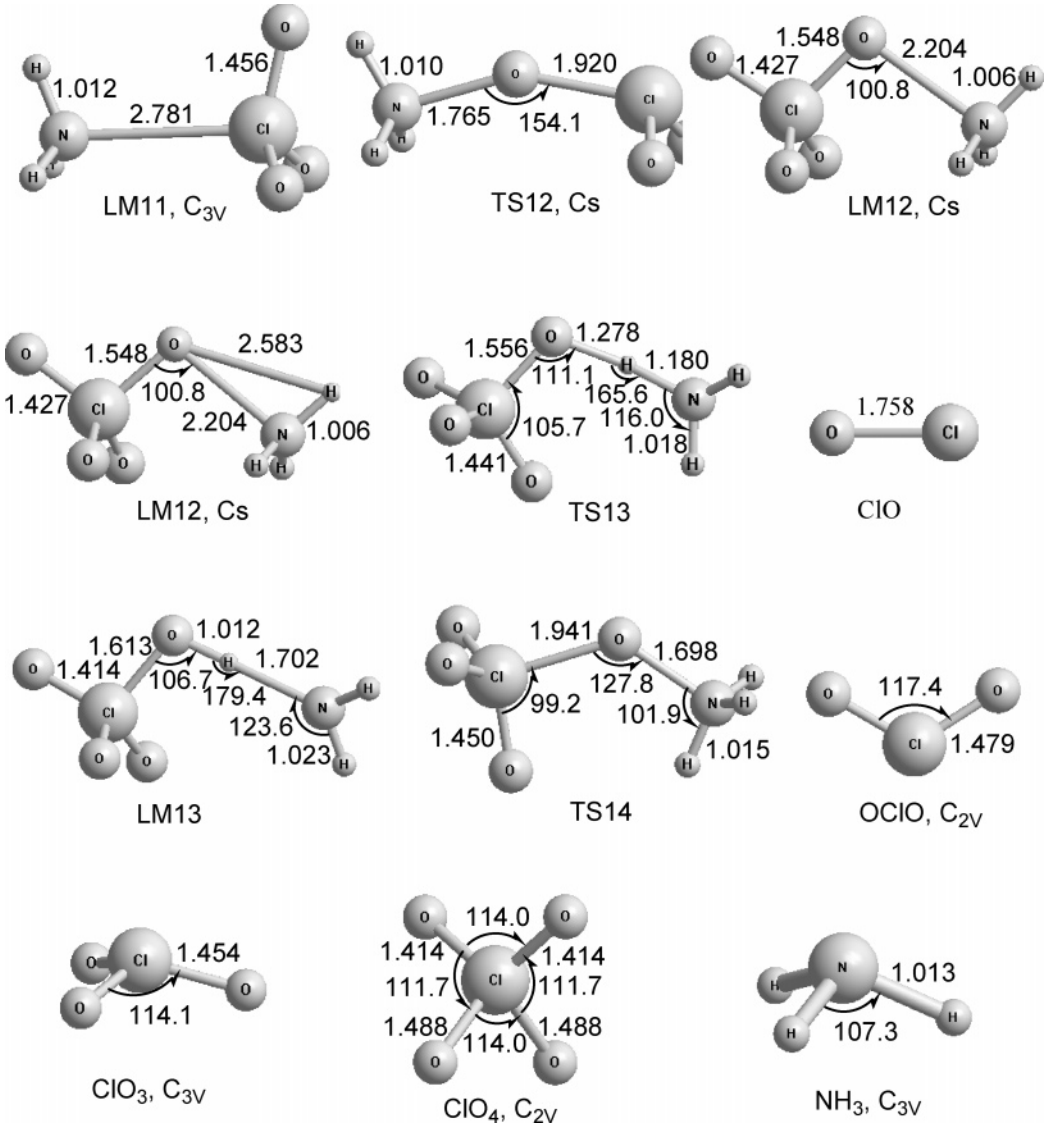

Figure 1. Geometric parameters (lengths in ånstroms and angles in degrees) of the reactants, intermediate complexes, and transition states optimized at the B3LYP/6-311+G(3df,2p) level of theory.

III. Results and Discussion

A. Mechanisms of $NH_3 + ClO_x$ ($x = 0-4$) Reactions. The optimized geometries of the intermediate complexes and transition states at the B3LYP/ 6-311+G(3df,2p) level of theory are shown in Figure 1; all their Cartesian coordinates and vibrational frequencies are placed in Table S1 of the Supporting Information. The vibrational frequencies and moments of inertia of reactants and some of their intermediate complexes and transition states used in the rate constant calculation are listed in Table 1. The potential energy diagrams of the five reactions, obtained at the G2M//B3LYP/6-311+G(3df,2p) level of theory, are presented in Figure 2. Otherwise stated, all the energies cited below are the G2M values relative to those of the reactants. In addition, the spin−orbit correction, −0.83 kcal/mol, is included for the Cl atom[12] in the potential energy diagram for the NH_3 + Cl reaction.

NH_3 + Cl. As shown in Figures 1 and 2, there are two possibilities for Cl atom to attack the NH_3 molecule. In the first case, Cl approaches the side of the H atoms in NH_3 to form an NH_3...Cl hemibonded complex (LM1) with C_{3v} symmetry; the Cl−H separation is 2.595 Å. LM1 lies 3.6 kcal/mol below the reactants; it can eliminate an HCl molecule via TS1 with a 7.8 kcal/mol barrier above LM1. On the product side, another H-bonded complex $H_2N\cdots HCl$ (LM2) was located, which is 4.0 kcal/mol lower than the final products, NH_2 + HCl. Also, at the B3LYP/6-311+G(3df,2p) level of theory, the energy of LM1 is 12.0 kcal/mol below that of reactants, which is 8.4 kcal/mol greater than that at the G2M level. This extra stability may be caused by overestimating the electron correlation energy of the hemibonded complex by the density functional theory. In the second case, Cl approaches the N atom of NH_3 to form a more stable intermediate complex $Cl\cdots NH_3$ (LM3) with the binding energy of 7.1 kcal/mol and the Cl−N bonding distance of 2.432 Å. However, the further decomposition of LM3 to NH_2-Cl + H needs to pass TS2 with a much higher potential barrier of 48.7 kcal/mol.

From Figure 2, the heats of reaction for the formation of NH_2 + HCl and NH_2Cl + H are predicted to be 4.6 and 46.8 kcal/mol, respectively. On the basis of the heats of formation for NH_3, NH_2, Cl, HCl, and H tabulated by Chase[13] in 1998, the heat of reaction of $NH_3 + Cl \rightarrow NH_2 + HCl$ is 4.8 ± 1.5 kcal/mol. The predicted value lies within the experimental error range. Also, on the basis of the two values of the heat of formation of NH_2Cl given by Livett et al.,[14] 17.7 kcal/mol (obtained from 16 kcal/ mol at 298 K based on the heats of formation of NH_2^+ and Cl) and 13.7 kcal/mol (obtained from

TABLE 1: Vibrational Frequencies and Moments of Inertia for the Reactants, Some Intermediates, and Transition States of the $NH_3 + ClO_x$ ($x = 0-4$) Reactions Computed at the B3LYP/6-311+G(3df,2p) Level of Theory

species	moments of inertia (au)	frequencies (cm^{-1})
NH_3 ($^1A_1$)	6.0, 6.0, 9.5	1022, 1665, 1665, 3481, 3599, 3599
ClO ($^2\Pi_1$)	97.3, 97.3	861
OClO ($^2B_1$)	35.2, 182.4, 217.7	450, 965, 1116
ClO_3 ($^2A_1$)	179.3, 179.3, 340.0	471, 471, 564, 921, 1078, 1078
ClO_4 ($^2B_1$)	297.4, 318.6, 342.3	375, 385, 414, 549, 573, 647, 903, 1161, 1258
LM1	10.6, 268.3, 268.3	223, 371, 384, 398, 1580, 1581, 3544, 3736, 3737
LM2	4.7, 424.0, 428.8	162, 175, 198, 607, 629, 1520, 2550, 3395, 3490
LM4	82.8, 647.8, 721.7	36, 56, 92, 122, 213, 868, 1037, 1664, 1673, 3470, 3585, 3595
LM5	76.9, 543.7, 620.6	30, 75, 217, 252, 293, 733, 746, 1442, 1527, 3401, 3410, 3498
LM7	134.3, 687.4, 812.1	46, 60, 65, 99, 186, 233, 456, 960, 1066, 1103, 1664, 1667, 3475, 3589, 3590
LM8	197.1, 612.2, 731.8	30, 84, 104, 226, 274, 344, 358, 665, 861, 965, 1412, 1525, 3266, 3405, 3501
LM9	344.0, 558.9, 558.9	89, 91, 133, 172, 258, 288, 479, 479, 526, 766, 893, 1008, 1008, 1607, 1608, 3466, 3648, 3648
LM10	311.4, 723.8, 760.8	19, 57, 82, 227, 263, 336, 394,442, 543, 671, 818, 1036, 1158, 1382, 1518, 3074, 3407, 3506
LM12	339.7, 761.9, 770.5	30, 98, 126, 287, 388, 413, 425,439, 486, 586,587, 600, 759, 1004, 1190, 1204, 1572, 1590, 3509, 3698, 3720
LM13	339.8, 948.6, 964.1	25, 33, 68, 231, 303, 368, 414, 444, 571, 582, 586, 747, 902, 1038, 1231, 1262, 1477, 1525, 2961, 3416, 3513
TS1	6.7, 327.7, 330.6	*i*319, 347, 429, 740, 911, 1414, 1589, 3411, 3508
TS3	61.1, 456.8, 514.0	*i*1519, 137, 140, 415, 552, 676, 772, 1233, 1548, 1592, 3446, 3537
TS7	162.1, 598.2, 681.1	*i*740, 75, 95, 151, 364, 437, 532, 683, 977, 1076, 1268, 1505, 1588, 3436, 3533
TS11	281.9, 578.6, 635.5	*i*1170, 57, 142, 220, 400, 438,462, 514, 607, 680, 830, 968, 1114, 1370, 1483, 1594, 3470, 3576
TS13	331.6, 867.9, 876.1	*i*1182, 32, 108, 161, 305, 409, 420, 495, 558, 589, 612, 672, 844, 014, 1177, 1221, 1227, 1549, 1628, 3476, 3594

12 kcal/mol at 298 K using bond energy data obtained in their experiment) at 0 K, the heats of reaction for $NH_3 + Cl \rightarrow H + NH_2Cl$ are estimated to be 50.0 and 46.0 kcal/mol, respectively.

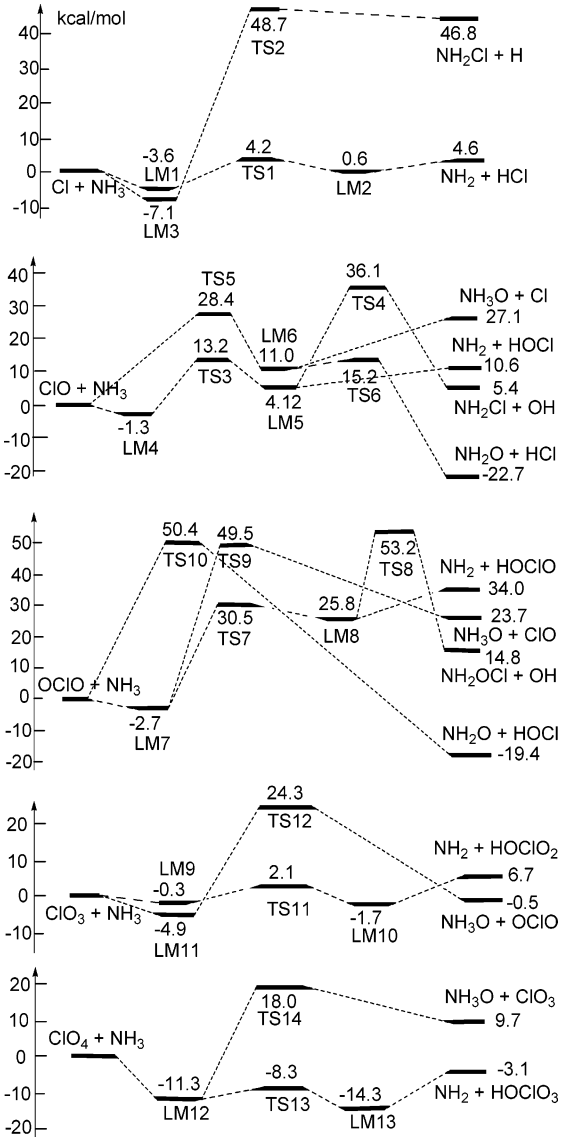

Figure 2. Schematic energy diagrams (in kcal/mol units) computed at the G2M//B3LYP/6-311+G(3df,2p) level of theory.

Our predicted value is 3.2 kcal/mol less than the former and is 0.8 kcal/mol higher than the latter. It is thus reasonable to employ the G2M method for elucidation and prediction of the kinetics and mechanisms of the $NH_3 + ClO_x$ reactions.

Comparing the PES of $NH_3 + Cl$, the geometric parameters of the transition state and complexes are basically in agreement with those optimized by Gao et al.[5] at the MPWB1K/6-31+G-(2df,2p) level of theory, and the energies of TS1, LM2, and LM3 are 2.5, 1.1, and 4.4 kcal/mol higher than theirs, respectively. However, they did not report the structure of the entrance complex (LM1) for the $NH_2 + HCl$ channel.

$NH_3 + ClO$. In this reaction, there are two possible reaction channels as shown in Figure 2. The first one is hydrogen atom abstraction from NH_3 by oxygen atom of ClO via a hydrogen-bond complex $ClO\cdots HNH_2$ (LM4) and transition state (TS3) to another H-bonding complex $ClOH\cdots NH_2$ (LM5). LM4 is predicted to have a binding energy of 1.3 kcal/mol, and TS3 and LM5 lie above the reactants at 13.2 and 4.1 kcal/mol, respectively. The complex $ClOH\cdots NH_2$ can therefore easily decompose to the products $NH_2 + HOCl$ followed by $H\cdots N$ bond breaking. Although LM5 can connect with the products $NH_2Cl + HO$ via TS4 with Cl atom attacking N atom, their formation is not expected to be important because of the much higher barrier of TS4 (36 kcal/mol).

The second reaction channel is the approaching of the O atom of ClO toward the N atom of NH_3 via TS5 with the Cl−O bond lengthening concertedly to give the complex LM6. The potential barrier of this step is 28.4 kcal/mol, which is greater than that of TS3 by 15.2 kcal/mol. LM6 is a four-membered ring structure with both weak Cl−O and Cl−H bonds. So, the Cl atom can be eliminated directly from LM6 to form $NH_3O + Cl$. In addition, the HCl molecule can be formed exothermically from LM6 via a much lower barrier at TS6, 4.3 kcal/mol above LM6 or 15.2 kcal/ mol above the $ClO + NH_3$ reactants. This direct NH_3 oxidation process cannot compete with the H-abstraction reaction producing HOCl in view of the high barrier at TS5.

$NH_3 + OClO$. Both reactants NH_3 and OClO can first form a four-membered ring complex (LM7) with 2.7 kcal/mol binding energy; the complex has a loose structure because of the long $O\cdots H$ and $Cl\cdots N$ separations in LM7 (see Figure 1). LM7 can undergo H-abstraction reaction via TS7 with a 30.5 kcal/mol barrier to form the complex $H_2N\cdots HOClO$ (LM8) and, in principle, can also undergo O-abstraction by NH_3 directly producing $NH_3O + ClO$ via TS9 with a much higher barrier of

49.5 kcal/mol. The latter process apparently cannot compete with the former due to its high barrier. LM8 is an N···H hydrogen-bonded complex lying slightly below TS7; it can dissociate readily to NH_2 + HOClO and, in principle, also to NH_2OCl + OH via a very high barrier at TS8, 53.2 kcal/mol, by a concerted dual-bond breaking process. In addition, a five-membered ring transition state TS10 can directly connect the reactants NH_3 + OClO with the lowest energy products NH_2O + HOCl. The potential barrier of TS10, 50.4 kcal/mol, is much higher than that of TS7 (30.5 kcal/mol), however, although it is the most exothermic process ($\Delta H = -19.4$ kcal/mol) in the system.

NH_3 + ClO_3. Similar to the NH_3 + Cl reaction, two prereaction complexes can be formed by H−O and N−Cl bondings giving LM9 and LM11, respectively. Both have C_{3v} structures with energies slightly below the reactants by 0.3 and 4.9 kcal/mol, respectively, as shown in Figure 2. From LM9, the shortening of one of the three H···O bonds with the concurrent lengthening of the associated H−N bond at TS11 gives rise to the H-abstraction product LM10, an N···H-bonding complex, H_2N···$HOClO_2$. LM10 can further fragment to produce the final products NH_2 + $HOClO_2$ with an overall 6.7 kcal/mol endothermicity. The energy of TS11 is 2.1 kcal/mol while that of LM10 is −1.7 kcal/mol. This H-abstraction reaction can take place readily.

Another reaction channel is from LM11 to products NH_3O + OClO via the oxygen abstraction transition state TS12 with a 24.3 kcal/mol barrier. Because TS12 is about 12 times greater than TS11 in energy, this redox process is kinetically irrelevant.

NH_3 + ClO_4. Because of the C_{2v} symmetry of ClO_4 in the ground electronic state ($^2B_1$), it can only form one intermediate complex (LM12) with NH_3 as seen in Figure 2. The prereaction complex has a 11.3 kcal/mol binding energy. Similar to the NH_3−ClO_2 system, both H- and O-abstraction reactions can ensue from LM12. H-abstraction occurs via TS13 to give a stable H_2N···$HOClO_3$ complex (LM13, −14.3 kcal/mol below the reactants) and the final products NH_2 + $HOClO_3$. Because of the small abstraction barrier and the high stabilities of both LM12 and LM13, TS13 lies below the reactants by as much as 8.3 kcal/mol, or 3.0 and 6.1 kcal/mol above LM12 and LM13, respectively. The reaction producing NH_2 + $HOClO_3$ is exothermic ($\Delta H = -3.1$ kcal/mol), and it can take place readily.

The barrier for O-transfer from ClO_4 to NH_3 via TS14 is 18.0 kcal/mol, which is much greater than that for the H-abstraction process. Thus, the direct oxidation of NH_3 to NH_3O by ClO_4 is unimportant.

From the above discussions of the five reaction mechanisms, we can conclude that H-abstraction is the most favorable path in each reaction; the amidogen radical (NH_2) is therefore the main product in this series of reactions. Comparing the reaction barriers for all the H-abstraction channels, the following decreasing order with OClO > ClO > Cl > ClO_3 > ClO_4 is observed. Also, from the five N···H hydrogen-bonding complexes, LM2, LM5, LM8, LM10, and LM13, the N···H bond energies are predicted to be 4.0, 6.5, 8.2, 8.4, and 11.3 kcal/mol, respectively. Obviously, the N···H bond strengths increase with the number of oxygen atoms in $HClO_x$ ($x = 0-4$). At the B3LYP/6-311+G(3df,2p) level of theory, the Mulliken atomic charge of N in NH_2 is −0.386e while those of Cl in HCl, HOCl, HOClO, $HOClO_2$, and $HOClO_3$ are −0.220e, 0.029e, 0.528e, 0.968e, and 1.714e, respectively. Accordingly, the variation in the N···H bond strengths may be attributed to the atomic charges of Cl in $HClO_x$. The more positive the Mulliken atomic charge of Cl in $HClO_x$ is, the stronger the N···H bond in the complex H_2N···$HClO_x$ becomes.

TABLE 2: Morse Parameters for Association/Dissociation Processes of the Hydrogen Abstraction Channels

reaction	D_e/kcal/mol	β/Å^{-1}	R_e/Å
LM1 → NH_3 + Cl	4.4	1.654	2.595
LM2 → NH_2 + ClO	6.0	1.423	1.890
LM5 → NH_2 + HOCl	8.6	1.474	1.836
LM8 → NH_2 + HOClO	10.1	1.880	1.803
LM10 → NH_2 + $HOClO_2$	10.4	1.370	1.759
LM12 → NH_3 + ClO_4	13.4	1.671	2.204
LM13 → NH_2 + $HOClO_3$	13.2	1.513	1.702

B. Rate Constant Calculations. As discussed in the above section, the hydrogen abstractions from NH_3 by ClO_x ($x = 0-4$) take place by complex-forming metathetical mechanisms involving H-bonding prereaction and postreaction intermediates:

$$Cl + NH_3 \leftrightarrow LM1 \leftrightarrow TS1 \leftrightarrow LM2 \rightarrow NH_2 + HCl \quad (1)$$

$$ClO + NH_3 \leftrightarrow LM4 \leftrightarrow TS3 \leftrightarrow LM5 \rightarrow NH_2 + HOCl \quad (2)$$

$$OClO + NH_3 \leftrightarrow LM7 \leftrightarrow TS7 \leftrightarrow LM8 \rightarrow NH_2 + HOClO \quad (3)$$

$$ClO_3 + NH_3 \leftrightarrow LM9 \leftrightarrow TS10 \rightarrow NH_2 + HOClO_2 \quad (4)$$

$$ClO_4 + NH_3 \leftrightarrow LM12 \leftrightarrow TS13 \leftrightarrow LM13 \rightarrow NH_2 + HOClO_3 \quad (5)$$

The rate constants of these processes were calculated by microcanonical VTST and RRKM theory (for reaction 5), and the contributions from other channels are reasonably neglected. The VTST calculations were carried out with the unified statistical formulation of Miller[15] including both tunneling and multiple reflection corrections[16] above the shallow wells of the prereaction and postreaction complexes. For the RRKM calculations, the L-J (Lennard-Jones) parameters were taken to be σ = 3.47 Å and ϵ/k = 114 K for argon buffer gas from the literature[17] and σ = 4.20 Å and ϵ/k = 230 K approximately for the intermediate complexes from our previous paper[18] on the HOOClO molecular intermediate. The minimum energy paths (MEPs) for barrierless association and dissociation processes occurring without intrinsic transition states were optimized at the B3LYP/6-311+G(3df, 2p) level of theory by manually varying the key coordinates point by point for complex formation from the reactants or products. They were fitted to Morse functions to approximately represent the MEPs of the association/dissociation processes. The Morse parameters are summarized in Table 2.

As indicated above, the Eckart tunneling corrections[19] have been made for rate constants of the H-abstraction reactions at low temperatures. However, only NH_3 + ClO and NH_3 + ClO_3 reactions have noticeable tunneling effects because of their larger imaginary frequencies, 1519 cm^{-1} at TS3 and 1170 cm^{-1} at TS11. Their rate constants with Eckart tunneling corrections are 91.9% and 37.3% larger at 300 K for the former and latter processes, respectively. For the NH_3 + Cl reaction the correction only increases its rate constant by 1.2% at 300 K because of the smaller imaginary frequencies, 319 cm^{-1} at TS1. The tunneling effects on the other two reactions are negligibly small.

The effects of multiple reflections above the complex-wells predicted with Miller's method[15] show that the rate constants for H-abstraction reactions by ClO, OClO, and ClO_4 are reduced by 44.8%, 172.0%, and 59.5%, respectively, at 300 K. The rate constant of NH_3 + Cl was decreased by only 17.6%, and that

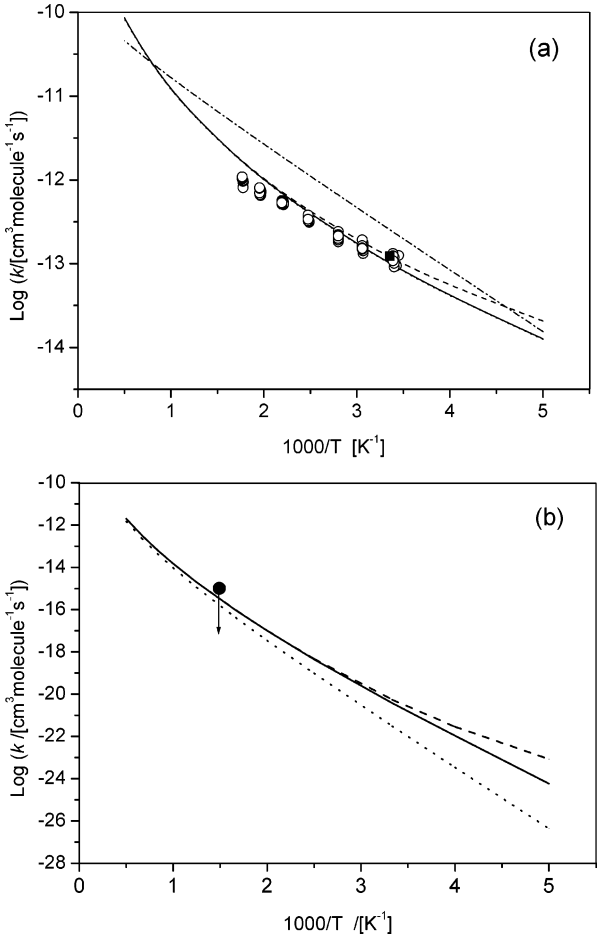

Figure 3. Predicted rate constants with multiple reflection and tunneling corrections comparing with the experimental data: (a) k (NH_3 + Cl), (b) k (NH_3 + ClO). Solid line indicates rate constant with multiple reflection and tunneling effects. Dashed line indicates rate constant without multiple reflections. Dotted line indicates rate constant without tunneling corrections. Solid circle reflects ref 3. Solid square reflects ref 4. Open circle reflects experimental data from ref 5. Dashed−dotted line shows theoretical data from ref 5.

of NH_3 + ClO_3 was not affected at 300 K. These effects stem primarily from the multiple reflections above the wells of postreaction complexes as their H-abstraction transition states are closer to the exit variational barriers leading to product formation. The effects of multiple reflection and tunneling corrections for the rate constants of the NH_3 + Cl and ClO reactions are shown in Figure 3. As shown in the figure, both tunneling and multireflection effects diminish gradually with increasing temperature.

In additon, the small-curvature effect[20a] on the reaction path of the smallest system, NH_3 + Cl, via the transition state TS1 was included to correct the hydrogen transfer rate constant. The small-curvature correction factors were predicted to be 3.99 and 1.62 at 300 and 500 K, respectively; the effect disappears at high temperatures. It can also be ignored in larger reaction systems.

Figure 4 compares the rate constants of these five reactions in the temperature range 200−2000 K. All rate constants have small positive temperature dependence and exhibit no pressure effect, except that for the NH_3 + ClO_4 reaction which has a small negative temperature dependence with a minor pressure effect at low temperatures above 100 atm. Because of the existence of the large pre- and postreaction complexes in this reaction, we have also performed rate constant calculations at 300, 500, 800, and 1000 K temperatures using the ChemRate

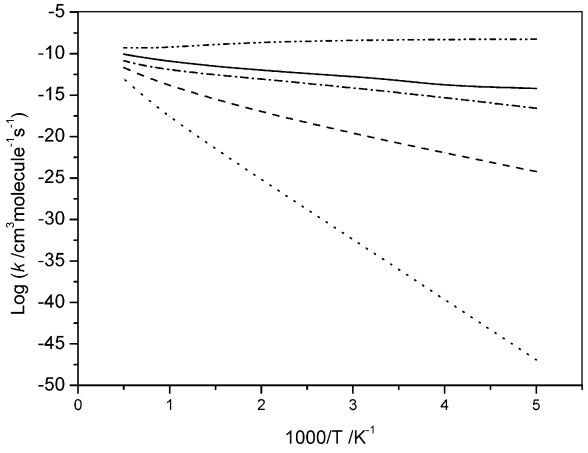

Figure 4. Predicted rate constants for five hydrogen abstraction reactions. Solid line shows k(NH_3 + Cl). Dashed line shows k(NH_3 + ClO). Dotted line shows k(NH_3 + OClO). Dashed−dotted line indicates k(NH_3 + ClO_3). Dashed−double-dotted line indicates k(NH_3 + ClO_4).

TABLE 3: Comparison of Predicted Rate Constants k_C (by ChemRate Program) and k_V (by Variflex Program) in cm^3 $molecule^{-1}$ s^{-1} for Reaction 5: $ClO_4 + NH_3 \leftrightarrow$ LM12 $\leftrightarrow$TS13 $\leftrightarrow$ LM13 $\rightarrow NH_2 + HOClO_3$

T (K)	k_C	k_V
300	2.44×10^{-9}	3.09×10^{-9}
500	1.32×10^{-9}	1.49×10^{-9}
800	3.51×10^{-10}	5.16×10^{-10}
1000	2.44×10^{-10}	3.78×10^{-10}

code[11] for comparison with the values predicted by Variflex.[9] The variational transition states for the barrierless association/decomposition pocesses were determined by the canonical variational method.[16a,20] The results of these calculations summarized in Table 3 indicated that the agreement in the values obtained by both methods is quite good.

The predicted individual rate constants at atmospheric pressure in units of cm^3 $molecule^{-1}$ s^{-1} can be expressed as

$$k(NH_3 + Cl) = 9.11 \times 10^{-19} T^{2.47} \exp(-726/T)$$

$$k(NH_3 + ClO) = 1.87 \times 10^{-24} T^{3.85} \exp(-4344/T)$$

$$k(NH_3 + OClO) = 1.48 \times 10^{-20} T^{3.05} \exp(-15657/T)$$

$$k(NH_3 + ClO_3) = 1.36 \times 10^{-14} T^{1.01} \exp(-2255/T)$$

$$k(NH_3 + ClO_4) = 8.44 \times 10^{-1} T^{-3.02} \exp(-528/T) \quad (200-1000\ K)$$

$$= 2.34 \times 10^{-20} T^{2.80} \exp(4392/T) \quad (1000-2000\ K)$$

As mentioned in the Introduction, there are two experimental rate constant data available for the NH_3+Cl reaction: k(NH_3+Cl) = 1.23×10^{-13} cm^3 $molecule^{-1}$ s^{-1} at 298 K, reported by Westenberg and DeHaas,[4] and the expression k(NH_3+Cl) = $(1.08 \pm 0.05) \times 10^{-11} \exp[-(2.74 \pm 0.04\ kcal\ mol^{-1})/RT]$ cm^3 $molecule^{-1}$ s^{-1} for the temperature range 290−570 K, reported by Gao et al.[5] As mentioned previously, Gao et al.[5] also evaluated the theoretical rate constants from the PES calculated at the MPWB1K/6-31+G(2df,2p) level of theory. Figure 3a compares these data with our predicted result. Our predicted rate cosntants are in good agreeement with the experimental data below 500 K with a small deviation noted at higher

temperatures. The theoretical prediction by Gao et al. is, however, 2 times greater than their experimental values.

For the NH_3+ClO reaction, only one experimental rate constant, $k(NH_3+ClO) \leq 1 \times 10^{-15}$ cm^3 molecule^{-1} s^{-1}, describes an upper limit of the rate constant at 670 K by Clyne and Watson.[3] The value predicted at 670 K for this reaction, 3.04×10^{-16} cm^3 molecule^{-1} s^{-1}, is consistent with the experimental upper limit. For the $ClO_4 + NH_3$ reaction, the exceptionally large rate constant at low temperatures (see Table 3) results from the unique combination of the following factors: (1) the high attractive potential between ClO_4 and NH_3 (the $H_3N\cdots OClO_3$ complex has a very large dipole moment of 6.1362 D), (2) all the transition states involved in the reaction lie below the reactants, resulting in a downhill slide from the reactants to the products ($NH_2 + HOClO_3$), and (3) the large reaction path degeneracy, 12, for the abstraction reaction.

We believe that the above rate constants for the $NH_3 + ClO_x$ ($x = 0 - 4$) reactions are reasonable and may be employed for computer modeling of propellant combustion involving AP with a high degree of reliability within the temperature range specified.

IV. Conclusions

The mechanisms for a series of reactions of NH_3 with ClO_x ($x = 0 - 4$) radicals have been studied at the G2M//B3LYP/6-311+G(3df,2p) level of theory in conjunction with statistical rate-theory calculations. The results of these calculations show that the H-abstraction process is the most favorable low-energy reaction channel in each of these reactions, and the predicted barriers in declining order are OClO > ClO > Cl > ClO_3 > ClO_4. Their rate constants have been calculated in temperature range 200−2000 K by microcanonical VTST and/or RRKM theory with Eckart tunneling and multiple-reflection corrections. The results of the calculations indicate that the tunneling effects on both $NH_3 + ClO$ and ClO_3 reactions are significant, and the effects of multiple reflections above the wells of H-bonding complexes, primarily the postreaction complexes, in the NH_3 reactions with ClO, OClO, and ClO_4 at low temperatures are noticeable. The predicted results (for Cl and ClO reactions) are basically in agreement with available experimental data.

Acknowledgment. This work was supported by the Office of Naval Research under Grant N00014-02-1-0133. Acknowledgment is also made to the Cherry L. Emerson Center of Emory University for the use of its resources, which are in part supported by a National Science Foundation grant (CHE-0079627) and an IBM Shared University Research Award. M.C.L. gratefully acknowledges the support from Taiwan's National Science Council for a distinguished visiting professorship at the Center for Interdisciplinary Molecular Science, National Chiao Tung University, Hsinchu, Taiwan.

Supporting Information Available: Geometries of all complexes and transition states. This material is available free of charge via the Internet at http://pubs.acs.org.

References and Notes

(1) Mader, C. L. *Numerical Modeling of Explosives and Propellants*, 2nd ed.; CRC Press: New York, 1998.

(2) Ibitayo, O. O.; Mushkatel, A.; Pijawka, K. D. *J. Hazard. Mater., A* **2004**, *114*, 15.

(3) Clyne, M. A. A.; Watson, R. T. *J. Chem. Soc., Faraday Trans. 1* **1974**, *70*, 2250.

(4) Westenberg, A. A.; DeHaas, N. *J. Chem. Phys.* **1977**, *67*, 2388.

(5) Gao, Y.; Alecu, I. M.; Hsieh, P.-C.; Morgan, B. P.; Marshall, P.; Krasnoperov, L. N. *J. Phys. Chem. A* **2006**, *110*, 6844.

(6) Mebel, A. M.; Morokuma, K.; Lin, M. C. *J. Chem. Phys.* **1995**, *103*, 7414.

(7) (a) Becke, A. D. *J. Chem. Phys.* **1993**, *98*, 5648. (b) Becke, A. D. *J. Chem. Phys.* **1992**, *96*, 2155.(c) Lee, C.; Yang, W.; Parr, R. G. *Phys. Rev.* **1988**, *37B*, 785.

(8) Frisch, M. J.; Trucks, G. W.; Schlegel, H. B.; Scuseria, G. E.; Robb, M. A.; Cheeseman, J. R.; Montgomery, Jr., J. A.; Vreven, T.; Kudin, K. N.; Burant, J. C.; Millam, J. M.; Iyengar, S. S.; Tomasi, J.; Barone, V.; Mennucci, B.; Cossi, M.; Scalmani, G.; Rega, N.; Petersson, G. A.; Nakatsuji, H.; Hada, M.; Ehara, M.; Toyota, K.; Fukuda, R.; Hasegawa, J.; Ishida, M.; Nakajima, T.; Honda, Y.; Kitao, O.; Nakai, H.; Klene, M.; Li, X.; Knox, J. E.; Hratchian, H. P.; Cross, J. B.; Adamo, C.; Jaramillo, J.; Gomperts, R.; Stratmann, R. E.; Yazyev, O.; Austin, A. J.; Cammi, R.; Pomelli, C.; Ochterski, J. W.; Ayala, P. Y.; Morokuma, K.; Voth, G. A.; Salvador, P.; Dannenberg, J. J.; Zakrzewski, V. G.; Dapprich, S.; Daniels, A. D.; Strain, M. C.; Farkas, O.; Malick, D. K.; Rabuck, A. D.; Raghavachari, K.; Foresman, J. B.; Ortiz, J. V.; Cui, Q.; Baboul, A. G.; Clifford, S.; Cioslowski, J.; Stefanov, B. B.; Liu, G.; Liashenko, A.; Piskorz, P.; Komaromi, I.; Martin, R. L.; Fox, D. J.; Keith, T.; Al-Laham, M. A.; Peng, C. Y.; Nanayakkara, A.; Challacombe, M.; Gill, P. M. W.; Johnson, B.; Chen, W.; Wong, M. W.; Gonzalez, C.; Pople, J. A. *Gaussian 03, Revision C.01*; Gaussian, Inc.: Wallingford CT, 2004.

(9) Klippenstein, S. J.; Wagner, A. F.; Dunbar, R. C.; Wardlaw, D. M.; Robertson, S. H. *VARIFLEX*, version 1.00; Argonne National Laboratory, 1999.

(10) (a) Wardlaw, D. M.; Marcus, R. A. *Chem. Phys. Lett.* **1984**, *110*, 230. (b) Wardlaw, D. M.; Marcus, R. A. *J. Chem. Phys.* **1985**, *83*, 3462. (c) Klippenstein, S. J. *J. Chem. Phys.* **1992**, *96*, 367. (d) Klippenstein, S. J.; Marcus, R. A. *J. Chem. Phys.* **1987**, *87*, 3410.

(11) Mokrushin, V.; Bedanov, V.; Tsang, W.; Zachariah, M.; Knyazev, V. *ChemRate*, version 1.19; NIST: Gaithersburg, MD, 2002.

(12) Curtiss, L. A.; Raghavachari, K.; Redfern, P. C.; Rassolov, V.; Pople, J. A. *J. Chem. Phys.* **1998**, *109*, 7764.

(13) Chase, Jr, M. W. *NIST-JANAF Thermochemical Tables*, 4th ed; AIP, NSRDS: Woodbury, New York, 1998.

(14) Livett, M. K.; Nagy-Felsobuki, E.; Peel, J. B.; Willett, G. D. *Inorg. Chem.* **1978**, *17*, 1608.

(15) Miller, W. H. *J. Chem. Phys.* **1976**, *65*, 2216.

(16) (a) Chakraborty, D.; Hsu, C.-C.; Lin, M. C. *J. Chem. Phys.* **1998**, *109*, 8887. (b) Xu, Z. F.; Hsu, C.-H.; Lin, M. C. *J. Chem. Phys. A* **2005**, *122*, 234308. (c) Xu, S.; Zhu, R. S.; Lin, M. C. *Int. J. Chem. Kinet.* **2006**, *38*, 322.

(17) Hippler, H.; Troe, J.; Wendelken, H. J. *J. Chem. Phys.* **1983**, *78*, 6709.

(18) Xu, Z. F.; Zhu, R. S.; Lin, M. C. *J. Phys. Chem. A* **2003**, *107*, 1040.

(19) Eckart, C. *Phys. Rev.* **1930**, *35*, 1303.

(20) (a) Truhlar, D. G.; Isaacson, A. D.; Garrett, B. C. In *The Theory of Chemical Reaction Dynamics*; Baer, M., Ed.; CRC Press: Boca Raton, FL, 1985; Vol. 4, pp 65−137. (b) Hsu, C.-C.; Mebel, A. M.; Lin, M. C. *J. Chem. Phys.* **1996**, *105*, 2346.